NASA TECHNICAL NOTE

NASA TN D-6340

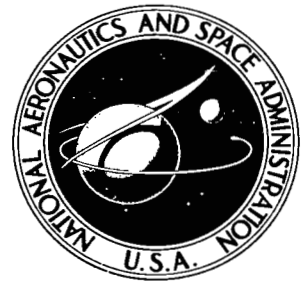

ACOUSTIC SCATTERING AND ABSORPTION BY A RIGID POROUS ELLIPTIC CYLINDRICAL SHELL

by William E. Zorumski

Langley Research Center
Hampton, Va. 23365

NATIONAL AERONAUTICS AND SPACE ADMINISTRATION • WASHINGTON, D. C. • AUGUST 1971

1. Report No.	2. Government Accession No.	3. Recipient's Catalog No.
NASA TN D-6340		

4. Title and Subtitle	5. Report Date
ACOUSTIC SCATTERING AND ABSORPTION BY A RIGID POROUS ELLIPTIC CYLINDRICAL SHELL	August 1971
	6. Performing Organization Code
7. Author(s)	8. Performing Organization Report No.
William E. Zorumski	L-7668
	10. Work Unit No.
9. Performing Organization Name and Address	136-80-01-04
NASA Langley Research Center Hampton, Va. 23365	11. Contract or Grant No.
	13. Type of Report and Period Covered
12. Sponsoring Agency Name and Address	Technical Note
National Aeronautics and Space Administration Washington, D.C. 20546	14. Sponsoring Agency Code

15. Supplementary Notes

The material presented herein is based on a thesis entitled "Acoustic Scattering by a Porous Elliptic Cylinder With Nonlinear Resistance" submitted in partial fulfillment of the requirements for the degree of Doctor of Philosophy in Engineering Mechanics, Virginia Polytechnic Institute, Blacksburg, Virginia, March 1970.

16. Abstract

Solutions for scattering of a plane wave from a thin rigid porous elliptic cylindrical shell are found in terms of Mathieu functions. The scattering problem reduces to an infinite set of linear equations for the coefficients of the velocity expansion on the cylindrical surface. Coupling terms in these equations are given by integrals which are evaluated by exact methods. Solutions are found by the method of reduction for the internal standing waves and the external scattered waves. A special case of variable acoustic impedance is found where the infinite systems uncouple so that closed-form solutions may be obtained for the velocity coefficients. Computations are made for scattering in the intermediate frequency range, where the wavelength is of the same order of magnitude as the major axis of the cylinder. Tabulations of the scattered and dissipated energies are given for various cylinder eccentricities, impedances, angles of incidence, and frequencies.

17. Key Words (Suggested by Author(s))	18. Distribution Statement
Acoustics Scattering Elliptic cylinders	Unclassified – Unlimited

19. Security Classif. (of this report)	20. Security Classif. (of this page)	21. No. of Pages	22. Price*
Unclassified	Unclassified	30	$3.00

*For sale by the National Technical Information Service, Springfield, Virginia 22151

ACOUSTIC SCATTERING AND ABSORPTION BY A RIGID POROUS ELLIPTIC CYLINDRICAL SHELL*

By William E. Zorumski
Langley Research Center

SUMMARY

Solutions for scattering of a plane wave from a thin rigid porous elliptic cylindrical shell are found in terms of Mathieu functions. The scattering problem reduces to an infinite set of linear equations for the coefficients of the velocity expansion on the cylindrical surface. Coupling terms in these equations are given by integrals which are evaluated by exact methods. Solutions are found by the method of reduction for the internal standing waves and the external scattered waves. A special case of variable acoustic impedance is found where the infinite systems uncouple so that closed-form solutions may be obtained for the velocity coefficients. Computations are made for scattering in the intermediate frequency range, where the wavelength is of the same order of magnitude as the major axis of the cylinder. Tabulations of the scattered and dissipated energies are given for various cylinder eccentricities, impedances, angles of incidence, and frequencies.

INTRODUCTION

The problem of acoustic scattering from a porous cylinder originates from the contemporary need for methods to reduce noise from aircraft turbofan engines. In reference 1 Marsh has shown that a practical method for reducing noise from turbofan engines is to install "broad-band resonators" inside the engine nacelle. Because of considerations of weight, safety, and endurance, these resonators are usually made of thin porous sheets of material (either metallic or fiber-glass—plastic) which are fastened to a honeycomb wall structure. The cavities behind the porous sheet are usually about one-quarter wavelength deep, since this depth gives good absorbing qualities.

In general, the greater the exposed area of porous material, the more the sound is absorbed, so that engine designers must look for ways to alter the engine geometry to increase this area. Of course, this increase must be accomplished without upsetting the basic flow field within the engine, which presumably has already been optimized on a

*The material presented herein is based on a thesis entitled "Acoustic Scattering by a Porous Elliptic Cylinder With Nonlinear Resistance" submitted in partial fulfillment of the requirements for the degree of Doctor of Philosophy in Engineering Mechanics, Virginia Polytechnic Institute, Blacksburg, Virginia, March 1970.

performance basis. One approach to this problem has been to install thin porous double-walled radial spokes or circumferential rings in the engine. The optimum size (from the acoustical viewpoint) of these devices is not known, but it is reasonable to assume that their dimensions are of the same order of magnitude as the wavelength of the dominant tone. In cross section, such a spoke or ring would appear roughly as an ellipse.

The literature on diffraction is extensive. The reader interested in this subject should consult the important review article by Bouwkamp (ref. 2). More than 500 papers published between 1940 and 1954 are reviewed in Bouwkamp's article, and the application of Mathieu functions to diffraction problems is discussed. Briefly, Mathieu functions may be used in the study of diffraction (or scattering) from elliptic cylinders. The article indicates that research prior to 1954 was limited to studies of the problem of scattering from a strip or slit (cylinder with eccentricity 1). This scattering problem has also been studied with an integral equation formulation (ref. 3).

Since Bouwkamp's survey, several papers have been published which deal with cylinders having eccentricity less than 1. In 1963 Yeh discussed the problem of a penetrable strip in terms of a Mathieu function series (ref. 4), and Barakat (ref. 5) made a study of the elliptic cylinder with various eccentricities. Barakat considered the exterior problem by using the classical Dirichlet (sound soft) and Neumann (sound hard) boundary conditions. This work made use of recently computed tables by Barakat, Houston, and Levin (ref. 6). These tables are appropriate for scattering problems in the long-wavelength range. In 1964 Burke and Twersky (see refs. 7, 8, and 9) began investigations in which low-frequency approximations were used.

In reference 7 Burke considered the problem of a cylinder composed of fluid with a density different from that of the medium in which it is immersed. Boundary conditions at the surface of the elliptic cylinder were continuity of normal velocity and continuity of pressure. His paper, like Yeh's (ref. 4), considered the coupled interior and exterior cylinder problem. The analysis of this problem resulted in an infinite set of algebraic equations for the scattered waves. Burke indicated the connection between truncating these sets of equations and long-wavelength approximations. His series solution gave the far-field scattering amplitude up to the sixth power of the wave number, and the near-field amplitude (internal and external) up to the third power. Terms in the truncated equations could be evaluated from the previously mentioned tables of Barakat, Houston, and Levin (ref. 6), from the tables of Wiltse and King (refs. 10 and 11), or from computations based on known expansions of the Mathieu functions in terms of the other tabulated transcendental functions.

This paper considers the scattering of a plane wave from a porous cylindrical shell. The cylinder is a thin elliptic shell which is made of a rigid porous material. The solutions both inside and outside of the cylinder are obtained in a general form and expressed

in terms of the unknown velocity normal to the cylinder surface. It is assumed that this normal velocity is continuous at the cylinder surface and that the pressure differential is related to the normal velocity by the complex impedance of the porous material. This relation between pressure differential and velocity is used to find the solution for the velocity. With the velocity through the cylinder surface known, calculations may be made for other quantities such as scattered energy and pressures inside and outside of the cylinder.

SYMBOLS

A_r, B_r, C_r, D_r coefficients

b, be_r, bo_r characteristic values

$C_n^{\nu}(x)$ Gegenbauer polynomial

c speed of sound

$De_k^{(r)}$ Fourier coefficient of even periodic Mathieu function

$Do_k^{(r)}$ Fourier coefficient of odd periodic Mathieu function

DR ratio of dissipated to incident power

e base of natural system of logarithms, 2.718

$g(\xi,\eta) = h\sqrt{\cosh^2\xi - \cos^2\eta}$

$He_r^{(1)}(s,\xi) = Je_r(s,\xi) + iNe_r(s,\xi)$

$He_r^{(2)}(s,\xi) = Je_r(s,\xi) - iNe_r(s,\xi)$

$Ho_r^{(1)}(s,\xi) = Jo_r(s,\xi) + iNo_r(s,\xi)$

$Ho_r^{(2)}(s,\xi) = Jo_r(s,\xi) - iNo_r(s,\xi)$

h dimensionless focal length

i unit imaginary number

$Je_r(s,\xi), Jo_r(s,\xi)$ radial Mathieu functions of the first kind

J_n, Y_n Bessel functions of integer order

j,k,ℓ,m,n,p,r,ν integers

$$M_{\ell,r} = \int_0^{2\pi} \left[g(\xi_o,\eta)\right]^{-1} Se_\ell(s,\eta) Se_r(s,\eta) d\eta$$

$$N_{\ell,r} = \int_0^{2\pi} \left[g(\xi_o,\eta)\right]^{-1} So_\ell(s,\eta) So_r(s,\eta) d\eta$$

$$N_r = \int_0^{2\pi} \left[Se_r(s,\eta)\right]^2 d\eta$$

$$N_r' = \int_0^{2\pi} \left[So_r(s,\eta)\right]^2 d\eta$$

$Ne_r(s,\xi), No_r(s,\xi)$ radial Mathieu functions of the second kind

P dimensionless power

p dimensionless pressure

$\vec{q}$ dimensionless velocity

q_ξ component of velocity normal to surface, ξ = Constant

Re( ) real part of a complex number

$Se_r(s,\eta)$ even periodic Mathieu function

$So_r(s,\eta)$ odd periodic Mathieu function

SR ratio of scattered to incident power

$s = h^2$

t dimensionless time

U_r, V_r coefficients in series for $g(\xi_o,\eta)q_\xi(\xi_o,\eta)$

w	projected width of cylinder
x,y	dimensionless rectangular coordinates
Z	specific impedance of cylinder
α	angle of incidence
η	circumferential elliptical coordinate
ξ	radial elliptical coordinate
ξ_o	coordinate of cylinder surface
ρ	mass density
ϕ,ψ	solutions to Mathieu's equation and Mathieu's modified equation, respectively
ω	circular frequency

Subscripts:

d	dissipation in porous material
I	incident
p	incident plane waves
s	scattered waves

Superscripts:

i	inside of cylinder
o	outside of cylinder
(1)	denotes diverging waves
(2)	denotes converging waves

* complex conjugate

A single prime denotes a first derivative (except for N_r', which has been defined separately). Double primes denote a second derivative.

ANALYSIS

Governing Equations

Figure 1 shows the elliptical cylinder coordinates (ξ and η) which will be used to study scattering from an elliptic cylinder. These coordinates are defined by

$$\left.\begin{aligned} x &= h \cosh \xi \cos \eta \\ y &= h \sinh \xi \sin \eta \end{aligned}\right\} \tag{1}$$

As shown in figure 1, curves with ξ equal to a constant are ellipses with focal points at $x = \pm h$. Curves with η equal to a constant are hyperbolas with focal points which correspond to those of the ellipses.

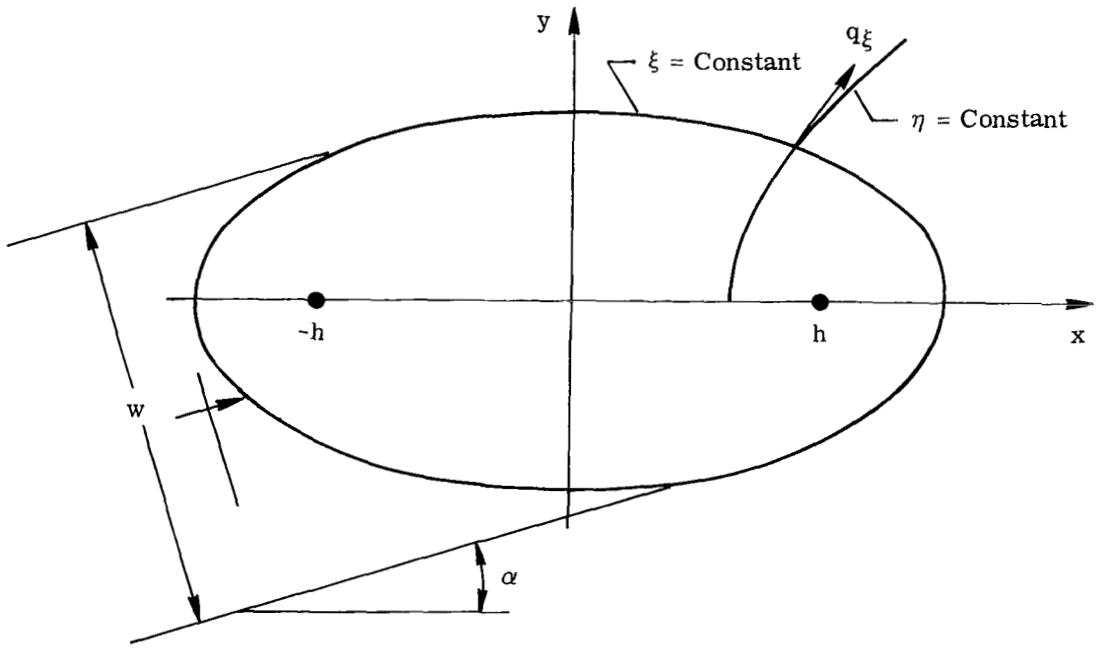

Figure 1.- Elliptical coordinates.

The problem being considered herein is the scattering of a plane wave from a porous cylinder whose surface corresponds to the elliptical coordinate ξ_o. This cylinder has a semimajor axis $h \cosh \xi_o$ and semiminor axis $h \sinh \xi_o$. The elliptical coordinates are naturally dimensionless quantities, and it is convenient to introduce dimensionless parameters for the other variables. Thus, h, p, $\vec{q}$, t, x, y, and Z are all defined as dimensionless parameters:

$$h = \frac{\omega \times \text{Focal length}}{c}$$

$$p = \frac{\text{Pressure}}{\rho c^2}$$

$$\vec{q} = \frac{\text{Velocity}}{c}$$

$$t = \omega \times \text{Time}$$

$$x = \frac{\omega \times \text{Longitudinal coordinate}}{c}$$

$$y = \frac{\omega \times \text{Lateral coordinate}}{c}$$

$$Z = \frac{\text{Impedance}}{\rho c}$$

The acoustic field equations are

$$\nabla^2 p + p = 0 \tag{2}$$

and

$$\vec{q} = -i\nabla p \tag{3}$$

where the time factor $\exp(-it)$ is understood.

The pressure and its gradient must be continuous inside and outside of the cylinder. Therefore, there are two continuity conditions at $\xi = 0$:

$$p^i(0,\eta) = p^i(0,-\eta) \tag{4a}$$

$$\frac{\partial p^i(0,\eta)}{\partial \xi} = \frac{-\partial p^i(0,-\eta)}{\partial \xi} \tag{4b}$$

At the surface of the porous cylinder, where $\xi = \xi_o$, there are two boundary conditions which relate the internal and external pressure fields. In order for mass to be conserved, the acoustic velocity normal to the cylinder surface must be continuous; that is,

$$q_{\xi}^{i}(\xi_o,\eta) = q_{\xi}^{o}(\xi_o,\eta) \tag{5}$$

However, there will be a pressure drop at the cylinder surface due to viscous dissipation and inertial effects within the porous material. This pressure drop is related to the acoustic velocity through the specific impedance of the material Z; that is,

$$p^{i}(\xi_o,\eta) - p^{o}(\xi_o,\eta) = Zq_{\xi}(\xi_o,\eta) \tag{6}$$

The field equations in elliptical coordinates become

$$\frac{\partial^2 p}{\partial \xi^2} + \frac{\partial^2 p}{\partial \eta^2} + h^2(\cosh^2\xi - \cos^2\eta)p = 0 \tag{7}$$

and

$$q_{\xi} = -i\left[g(\xi,\eta)\right]^{-1}\frac{\partial p}{\partial \xi} \tag{8}$$

Separating variables in equation (7) by letting

$$p(\xi,\eta) = \psi(\xi)\phi(\eta) \tag{9}$$

gives

$$\phi''(\eta) + (b - s\cos^2\eta)\phi(\eta) = 0 \tag{10}$$

and

$$\psi''(\xi) - (b - s\cosh^2\xi)\psi(\xi) = 0 \tag{11}$$

where

$$s = h^2 \tag{12}$$

Since the dimensionless parameter h is proportional to frequency, s is proportional to frequency-squared.

Equations (10) and (11) are called Mathieu's equation and Mathieu's modified equation, respectively. The solution ϕ of equation (10) must be a periodic function of η, of period π or 2π; the parameter b, which is a function of s, must be one of a countably infinite set of characteristic values for every s. Fourier series representations

of these periodic solutions are given by equations (40) to (43) in the appendix. These solutions form a complete orthogonal set

$$\left.\begin{aligned} \int_0^{2\pi} \mathrm{Se}_r(s,\eta)\mathrm{Se}_l(s,\eta)d\eta &= 0 \qquad (l \neq r) \\ &= N_r \qquad (l = r) \end{aligned}\right\} \tag{13a}$$

$$\left.\begin{aligned} \int_0^{2\pi} \mathrm{So}_r(s,\eta)\mathrm{So}_l(s,\eta)d\eta &= 0 \qquad (l \neq r) \\ &= N_r' \qquad (l = r) \end{aligned}\right\} \tag{13b}$$

For each characteristic value, there are two independent solutions of equation (11). These solutions are called radial solutions, or hyperbolic cylinder functions. Series representations of these solutions are given in reference 12.

Solution for Scattering From Cylinder

In terms of the notation of reference 12, the general equation for the pressure field is

$$p(\xi,\eta) = \sum_{r=0}^{\infty} \left\{ \left[A_r^{(1)} \mathrm{He}_r^{(1)}(s,\xi) + A_r^{(2)} \mathrm{He}_r^{(2)}(s,\xi) \right] \mathrm{Se}_r(s,\eta) + \left[B_r^{(1)} \mathrm{Ho}_r^{(1)}(s,\xi) + B_r^{(2)} \mathrm{Ho}_r^{(2)}(s,\xi) \right] \mathrm{So}_r(s,\eta) \right\} \tag{14}$$

The asymptotic expansions of the radial solutions show that solutions with the superscript (1) are diverging waves while the superscript (2) indicates converging waves.

It is often convenient to work with the real and imaginary parts of the radial solutions. In reference 12, the radial solutions are given as

$$\mathrm{He}_r^{(1)}(s,\xi) = \mathrm{Je}_r(s,\xi) + i\mathrm{Ne}_r(s,\xi) \tag{15a}$$

and

$$\mathrm{Ho}_r^{(1)}(s,\xi) = \mathrm{Jo}_r(s,\xi) + i\mathrm{No}_r(s,\xi) \tag{15b}$$

The Wronskian of these solutions is 1; that is

$$Je_r Ne_r' - Ne_r Je_r' = 1 \tag{16a}$$

and

$$Jo_r No_r' - No_r Jo_r' = 1 \tag{16b}$$

It can be shown that, in order for the pressure and velocity to be continuous at $\xi = 0$, the pressure inside the cylinder must be

$$p^i(\xi,\eta) = \sum_{r=0}^{\infty} \left[A_r^i Je_r(s,\xi)Se_r(s,\eta) + B_r^i Jo_r(s,\xi)So_r(s,\eta)\right] \tag{17}$$

From succeeding equations, the dependence of the functions on the parameter s can be understood.

It is convenient to formulate the problem in terms of the normal velocity through the cylinder surface. An expansion for this velocity may be taken in the form

$$g(\xi_o,\eta)q_\xi(\xi_o,\eta) = \sum_{r=0}^{\infty} \left[U_r Se_r(\eta) + V_r So_r(\eta)\right] \tag{18}$$

so that a solution for the coefficients U_r and V_r is equivalent to finding the velocity distribution. With equations (8) and (18), it may be shown that equation (17) becomes

$$p^i(\xi_o,\eta) = i \sum_{r=0}^{\infty} \left[\frac{U_r Je_r(\xi_o)}{Je_r'(\xi_o)} Se_r(\eta) + \frac{V_r Jo_r(\xi_o)}{Jo_r'(\xi_o)} So_r(\eta)\right] \tag{19}$$

The pressure due to plane waves of unit amplitude moving along a line which is inclined at an angle α to the major axis may be represented by (refs. 13 and 14)

$$p_p(\xi,\eta) = \exp\left[i(x\cos\alpha + y\sin\alpha)\right] = \sqrt{8\pi} \sum_{r=0}^{\infty} (i)^r \left[\frac{Se_r(\alpha)}{N_r} Je_r(\xi)Se_r(\eta) + \frac{So_r(\alpha)}{N_r'} Jo_r(\xi)So_r(\eta)\right] \tag{20}$$

where $(x\cos\alpha + y\sin\alpha)$ is the normal distance from the origin to the wave front.

The pressure due to waves scattered from the cylinder may be given as

$$p_s(\xi,\eta) = \sum_{r=0}^{\infty} \left[C_r He_r^{(1)}(\xi) Se_r(\eta) + D_r Ho_r^{(1)}(\xi) So_r(\eta)\right] \tag{21}$$

The total pressure outside of the cylinder is the sum of equations (20) and (21); that is, $p_p + p_s$. If equation (8), used to calculate the normal velocity from the total pressure, is matched with the velocity expansion (eq. (18)), C_r and D_r may be eliminated from the expression for the external pressure, which becomes

$$p^o(\xi_o,\eta) = i \sum_{r=0}^{\infty} \left\{ \left[U_r \frac{He_r^{(1)}(\xi_o)}{He_r'^{(1)}(\xi_o)} Se_r(\eta) + V_r \frac{Ho_r^{(1)}(\xi_o)}{Ho_r'^{(1)}(\xi_o)} So_r(\eta) \right] \right.$$

$$\left. + \sqrt{8\pi}(i)^r \left[\frac{Se_r(\alpha)}{N_r He_r'^{(1)}(\xi_o)} Se_r(\eta) + \frac{So_r(\alpha)}{N_r' Ho_r'^{(1)}(\xi_o)} So_r(\eta) \right] \right\} \tag{22}$$

The interior-pressure solution (eq. (19)) and the exterior-pressure solution (eq. (22)) are each expressed in terms of the velocity at the cylinder surface. The pressure differential and velocity at the surface must satisfy equation (6) so that substituting equations (19), (22), and (18) into equation (6) and utilizing the orthogonality properties of the periodic Mathieu functions (Se_r and So_r) give the four infinite sets of equations

$$Z \sum_{r=0}^{\infty} M_{2l,2r} U_{2r} + \frac{N_{2l}}{Je_{2l}'(\xi_o) He_{2l}'^{(1)}(\xi_o)} U_{2l} = -\frac{i^{2l+1}\sqrt{8\pi} Se_{2l}(\alpha)}{He_{2l}'^{(1)}(\xi_o)} \tag{23}$$

$$Z \sum_{r=0}^{\infty} M_{2l+1,2r+1} U_{2r+1} + \frac{N_{2l+1} U_{2l+1}}{Je_{2l+1}'(\xi_o) He_{2l+1}'^{(1)}(\xi_o)} = -\frac{i^{2l+2}\sqrt{8\pi} Se_{2l+1}(\alpha)}{He_{2l+1}'^{(1)}(\xi_o)} \tag{24}$$

$$Z \sum_{r=0}^{\infty} N_{2l+1,2r+1} V_{2r+1} + \frac{N_{2l+1}' V_{2l+1}}{Jo_{2l+1}'(\xi_o) Ho_{2l+1}'^{(1)}(\xi_o)} = -\frac{i^{2l+2}\sqrt{8\pi} So_{2l+1}(\alpha)}{Ho_{2l+2}'^{(1)}(\xi_o)} \tag{25}$$

and

$$Z \sum_{r=0}^{\infty} N_{2l+2,2r+2} V_{2r+2} + \frac{N_{2l+2}' V_{2l+2}}{Jo_{2l+2}'(\xi_o) Ho_{2l+2}'^{(1)}(\xi_o)} = -\frac{i^{2l+3}\sqrt{8\pi} So_{2l+2}(\alpha)}{Ho_{2l+2}'^{(1)}(\xi_o)} \tag{26}$$

where $l = 0, 1, 2, \ldots$ and where $M_{l,r}$ and $N_{l,r}$ are integrals that are defined in the symbol list and evaluated in the appendix. These four infinite sets of equations give the coefficients of the velocity expansion on the cylinder surface $(U_r$ and $V_r)$. Once the velocity at the cylinder surface is obtained, the pressure or velocity at any point may be computed.

A Special Case of Variable Impedance

There is a special case of variable material impedance for which it is possible to obtain a simple algebraic expression for U_r and V_r instead of the infinite sets of equations. If

$$Z = g(\xi_o, \eta)Z' \tag{27}$$

where Z' is a constant, then

$$U_r = -\frac{i^{r+1}\sqrt{8\pi}Se_r(\alpha)Je_r'(\xi_o)}{N_r\left[1 + Z'Je_r'(\xi_o)He_r'^{(1)}(\xi_o)\right]} \tag{28}$$

and

$$V_r = -\frac{i^{r+1}\sqrt{8\pi}So_r(\alpha)Jo_r'(\xi_o)}{N_r'\left[1 + Z'Jo_r'(\xi_o)Ho_r'^{(1)}(\xi_o)\right]} \tag{29}$$

Scattering Formulas

Some quantities of interest are the incident power, the scattered and dissipated power, and the far-field root-mean-square pressure. The derivation of formulas for these quantities is tedious, but routine, and only the definitions and final results are given herein.

The projected width of the cylinder on the oncoming plane wave is

$$w = 2g(\xi_o, \alpha) \tag{30}$$

as shown in figure 1. Consider a section of the cylinder whose dimensionless length $\left(\frac{\omega \times \text{Length}}{c}\right)$ is 1. The power due to the incident wave which passes through the projected area of this unit length of the cylinder is

$$P_p = \frac{w}{2\pi} \operatorname{Re} \int_0^{2\pi} \frac{|p_p|^2}{2} dt = \frac{w}{2} \tag{31}$$

In equation (31) a unit dimensionless length is being considered. The actual power for this length is found by multiplying equation (31) by the factor $\frac{\rho c^5}{\omega^2}$. The scattered power is

$$P_s = \frac{1}{2} \operatorname{Re} \int_0^{2\pi} p_s(\xi_o,\eta) q^*_{\xi,s}(\xi_o,\eta) g(\xi_o,\eta) d\eta \tag{32}$$

It may be shown that equation (32) reduces to

$$P_s = \frac{1}{2} \sum_{r=0}^{\infty} \left(|C_r|^2 N_r + |D_r|^2 N'_r \right) \tag{33}$$

where

$$C_r = \frac{1}{He'^{(1)}_r(\xi_o)} \left[iU_r - i^r \sqrt{8\pi} \frac{Se_r(\alpha)}{N_r} Je'_r(\xi_o) \right] \tag{34}$$

and

$$D_r = \frac{1}{Ho'^{(1)}_r(\xi_o)} \left[iV_r - i^r \sqrt{8\pi} \frac{So_r(\alpha)}{N'_r} Jo'_r(\xi_o) \right] \tag{35}$$

The power dissipated in the porous material is

$$P_d = \frac{1}{2} \operatorname{Re} \int_0^{2\pi} \left[p^i(\xi_o,\eta) - p^o(\xi_o,\eta) \right] g(\xi_o,\eta) q^*_\xi(\xi_o,\eta) d\eta$$

$$= \frac{1}{2} \operatorname{Re} \sum_{r=0}^{\infty} - \left\{ \frac{|U_r|^2 N_r}{Je'_r(\xi_o) He'^{(1)}_r(\xi_o)} + \frac{|V_r|^2 N'_r}{Jo'_r(\xi_o) Ho'^{(1)}_r(\xi_o)} \right.$$

$$\left. + i^{r+1} \sqrt{8\pi} \left[\frac{Se_r(\alpha) U^*_r}{He'^{(1)}_r(\xi_o)} + \frac{So_r(\alpha) V^*_r}{Ho'^{(1)}_r(\xi_o)} \right] \right\} \tag{36}$$

At large distances from the cylinder where $\xi >> 1$, the rms pressure p_{rms} is given by

$$\sqrt{he^{\xi}}p_{rms} \approx \left| \sum_{r=0}^{\infty} (-i)^r \left[C_r Se_r(\eta) - iD_{r+1} So_{r+1}(\eta) \right] \right| \tag{37}$$

RESULTS AND DISCUSSION

Scattering computations have been made for wavelengths that are of the same order of magnitude as the major axis of the cylinder. The longest wavelength considered is about three times the length of the major axis. The parameter s, which is proportional to the square of the frequency, is 4 for this low-frequency case. The shortest wavelength is about one-third the length of the major axis, which corresponds to $s = 100$.

The parameter ξ_0 determines the eccentricity of the cylinder. The ratio of the minor axis to the major axis of the cylinder is approximately equal to ξ_0 when ξ_0 is small. Computations have been made for values of ξ_0 of 0.2, 0.4, and 0.8. The largest value of ξ_0 gives a cylinder with a minor- to major-axis ratio of about 0.68.

For the frequencies considered in this paper, the Mathieu function series for the pressure and velocity fields were always sufficiently accurate with 14 terms, so it was necessary to evaluate Mathieu functions from order 0 to order 14.

Evaluation of both the periodic and radial Mathieu functions (ref. 12) depends on computing the coefficients $De_k^{(r)}$ and $Do_k^{(r)}$, which appear in the Fourier series given in the appendix. These coefficients are functions of the parameter s.

Evaluation of Mathieu Functions

Although the coefficients for the Mathieu functions are tabulated in reference 12 for the range of s used in this paper, it was easier to program the computer to use the characteristic values be_r and bo_r to compute these coefficients rather than to read and interpolate the tables of coefficients. The method given by Blanch in reference 15 was used for this computation. Results were checked against the tables of coefficients and were found to agree to eight significant figures. With this method of computation it is also possible to obtain the coefficients for $s > 100$ (which are not tabulated) from the tables of characteristic values for large s ($s > 100$) in reference 12. With the coefficients available, Fourier series could be used for computation of the periodic solutions.

The evaluation of the radial Mathieu functions depends on computing J_n and Y_n (Bessel functions of the first kind and second kind, respectively). The Bessel functions of the first kind were computed by Abramowitz's method (see ref. 16). In this method a unit value is assigned to J_k (where k is large compared with the argument of the

Bessel function), J_{k+1} is taken as zero, and then backward recurrence is used to find J_n for $n < k$. The normalization condition is then used to adjust the magnitude of the J_n's. The Bessel function Y_0 is obtained from its series representation in terms of J_n, Y_1 is found from the Wronskian relation, and the rest of the Y_n's are found by forward recurrence. Bessel functions computed by this method were accurate to nine or ten significant figures for the range of arguments used.

Because of the scarcity of tabulated data available on the radial Mathieu functions, these functions were calculated by two different methods. The Bessel function product series (eqs. 3.05 to 3.13 in ref. 12) was used; in addition, the Bessel function series (eqs. 3.03, 3.04, 3.15, and 3.16 in ref. 12) was used for comparison. The latter series involves Bessel functions with argument $\sqrt{s}\cosh\xi$. Each series was checked at the origin $(\xi_0 = 0)$ against the joining factors which are tabulated in reference 12. Also, each series was checked against the tables of Barakat, Houston, and Levin (ref. 6) and against the tables of Blanch and Clemm (ref. 17) for $s = 4$. This value was the upper limit (on s) of the available tables and the lower limit on s for this study.

The radial Mathieu functions of the first kind were the most difficult to evaluate. The Bessel function product series for $Je_0(4,0)$ checked against the National Bureau of Standards tables (ref. 12) to seven significant figures. However, this accuracy decreased to one significant figure for $Je_6(4,0)$, and functions of higher order could not be computed by this method. The accuracy of the product series for the $Je_r(s,\xi)$ and $Jo_r(s,\xi)$ functions increased with increasing s; $Je_0(100,0)$ was accurate to nine figures, and $Je_{14}(100,0)$ retained a two-figure accuracy.

The Bessel function series proved to be a superior method for computing Je_r and Jo_r. By this method $Je_0(4,0)$ was accurate to seven significant figures. Although this result was not an improvement over that obtained by using the product series, $Je_6(4,0)$ was found to be accurate to six significant figures, which represented an improvement of five significant figures, and $Je_8(4,0)$ was accurate to five significant figures. However, $Je_{10}(4,0)$ was accurate to only one significant figure, and $Je_{12}(4,0)$ and $Je_{14}(4,0)$ could not be computed. The accuracy of the Bessel function series for $Je_r(s,0)$ also tended to improve with increasing s; $Je_0(100,0)$ was accurate to six figures and $Je_{14}(100,0)$ was accurate to eight figures. Note that the higher order functions are more accurate than the lower order functions when s is large. This turns out to be a very important property, since, in the scattering problem, the long-wavelength ($s = 4$) solutions require only the lower order terms for convergence. The short-wavelength solutions ($s = 100$) require more terms, but it is no problem to compute these terms for the large values of s.

The radial Mathieu functions of the second kind were computed by the Bessel function product series. For $0 \leq r \leq 15$, $Ne_r(4,0)$ and $No_r(4,0)$ were accurate to eight

significant figures. The accuracy of the product series for $Ne_r(s,0)$ and $No_r(s,0)$ decreased with increasing s. For example, $Ne_0(100,0)$ was only accurate to three significant figures; $Ne_{14}(100,0)$ had six-figure accuracy, a loss of only two places.

The accuracy of both methods of computation improved with distance from the origin (increasing ξ_o). This fact was established by comparing the results of each series and assuming that, if they were the same, they were correct. Larger values of ξ correspond to smaller values of cylinder eccentricity; thus it is generally easier to evaluate the radial functions on a nearly circular cylinder than on a nearly flat cylinder.

In the problem of scattering from a porous cylinder, the Bessel function product series was used to evaluate the functions of the second kind and their derivatives. The Bessel function series was used to find the functions of the first kind, and the derivatives of these functions were found from the Wronskian relations (eqs. (16)).

The magnitude and phase of the complex radial Mathieu functions $He_r(s,\xi)$ and $Ho_r(s,\xi)$ could be computed to eight significant figures for $s = 4$, and to six figures for $s = 100$. This fact is somewhat surprising in view of the preceding discussion of the accuracy of the radial Mathieu functions of the first and second kinds which are, respectively, the real and imaginary parts of the complex function. The inaccurate (real) part of the complex number is much less in magnitude than the accurate (imaginary) part; thus, the complex representation of the number is fairly good throughout the range of s.

The evaluation of the coefficients in the scattering equations (eqs. (23) to (26)) depends directly on the evaluation of the Mathieu functions. The coefficients U_r and V_r in equations (23) to (26) are only as accurate as the radial functions of the first kind (Je_r and Jo_r) and their derivatives (Je_r' and Jo_r'). These quantities could be computed to at least five significant figures for $s = 4$ and orders up to eight. At $s = 100$ the functions of the first kind could be determined to at least six figures for all orders, but the functions of the second kind (Ne_r and No_r) could be obtained to only three figures for the lower orders. Since the Wronskian relations were used to solve for the derivatives, the derivatives of Je_r and Jo_r are limited to three-figure accuracy. The accuracy problem may be associated with the waves within the cylinder since this field is given in terms of radial functions of the first kind.

The nonhomogeneous terms in equations (23) to (26) may be computed to six significant figures since they involve only the complex radial functions and the periodic functions. The normalizing factors N_r and N_r' are computed from the coefficients $De_k^{(r)}$ and $Do_k^{(r)}$ and so are accurate to eight figures.

Computation of the coupling coefficients $M_{l,r}$ and $N_{l,r}$ is discussed in the appendix. The series presented therein were used to compute these coefficients. The integrals I_{2m} were computed to eight significant figures to obtain eight-figure accuracy for the coupling terms.

The four infinite sets of equations (eqs. (23) to (26)) were solved approximately by truncating the equations to a finite set. This method of solution, which is also called the method of reduction, is discussed in reference 18. Computations were made by using matrices of orders 5, 6, and 7, which gave 10, 12, and 14 terms, respectively, in the series for $q_{\xi}(\xi_o, \eta)$. It was observed that the numerical results did not change significantly as the order of the matrices increased to 7; this fact implies convergence of the solution by the method of reduction.

Scattering From a Porous Cylinder

Focal lengths h of 2, 4, 6, 8, and 10 were used to determine the effect of frequency on scattering and dissipation. These values correspond to lengths of the major axis of about one-half wavelength to over three wavelengths. Solutions were computed for real values of Z of 1, 2, and 4. The angle of incidence α was varied in 30^o increments from 0^o to 90^o, and the radial coordinate ξ_o was taken as 0.2, 0.4, and 0.8. Table I gives the ratios of scattered and dissipated power to incident power (SR and DR) for these conditions.

TABLE I.- SCATTERED AND DISSIPATED POWER RATIOS

(a) $h = 2.0$

ξ_o	α, deg	SR for $Z = 1.0$	DR for $Z = 1.0$	SR for $Z = 2.0$	DR for $Z = 2.0$	SR for $Z = 4.0$	DR for $Z = 4.0$
0.2	0	0.039	0.545	0.094	0.751	0.158	0.771
	30	.146	.599	.304	.635	.474	.542
	60	.294	.713	.601	.762	.946	.629
	90	.376	.721	.744	.770	1.179	.654
0.4	0	0.115	0.663	0.233	0.820	0.349	0.788
	30	.176	.694	.371	.792	.583	.695
	60	.275	.799	.583	.860	.936	.704
	90	.316	.828	.661	.869	1.609	.697
0.8	0	0.202	0.750	0.415	0.922	0.659	0.851
	30	.236	.730	.479	.866	.764	.771
	60	.321	.635	.612	.695	.938	.586
	90	.375	.553	.681	.570	1.008	.470

TABLE I.- SCATTERED AND DISSIPATED POWER RATIOS – Continued

(b) h = 4.0

ξ_o	α, deg	SR for Z = 1.0	DR for Z = 1.0	SR for Z = 2.0	DR for Z = 2.0	SR for Z = 4.0	DR for Z = 4.0
0.2	0	0.050	0.585	0.122	0.860	0.218	1.03
	30	.161	.647	.375	.797	.617	.763
	60	.312	.762	.654	.827	1.069	.697
	90	.365	.803	.740	.824	1.154	.653
0.4	0	0.138	0.693	0.298	0.927	0.483	0.956
	30	.202	.703	.437	.872	.742	.828
	60	.342	.655	.666	.707	1.038	.606
	90	.414	.597	.765	.604	1.139	.498
0.8	0	0.255	0.639	0.505	0.803	0.808	0.801
	30	.289	.619	.565	.728	.892	.694
	60	.324	.674	.642	.744	1.005	.652
	90	.392	.543	.718	.569	1.069	.499

(c) h = 6.0

ξ_o	α, deg	SR for Z = 1.0	DR for Z = 1.0	SR for Z = 2.0	DR for Z = 2.0	SR for Z = 4.0	DR for Z = 4.0
0.2	0	0.065	0.581	0.161	0.846	0.288	0.984
	30	.165	.670	.395	.852	.732	.835
	60	.320	.758	.666	.815	1.072	.674
	90	.390	.747	.760	.773	1.165	.621
0.4	0	0.181	0.590	0.377	0.728	0.599	0.697
	30	.236	.628	.496	.754	.828	.717
	60	.358	.637	.695	.685	1.076	.592
	90	.376	.722	.740	.742	1.137	.596
0.8	0	0.272	0.607	0.540	0.738	0.865	0.743
	30	.291	.632	.584	.734	.932	.700
	60	.340	.637	.661	.713	1.031	.649
	90	.377	.599	.706	.661	1.074	.605

TABLE I.- SCATTERED AND DISSIPATED POWER RATIOS – Concluded

(d) h = 8.0

ξ_o	α, deg	SR for Z = 1.0	DR for Z = 1.0	SR for Z = 2.0	DR for Z = 2.0	SR for Z = 4.0	DR for Z = 4.0
0.2	0	0.0692	0.454	0.171	0.636	0.308	0.710
	30	.174	.663	.415	.842	.773	.829
	60	.359	.667	.708	.716	1.109	.611
	90	.440	.609	.814	.596	1.207	.469
0.4	0	0.122	0.509	0.267	0.704	0.467	0.773
	30	.261	.596	.531	.713	.869	.704
	60	.343	.689	.682	.748	1.072	.638
	90	.424	.591	.785	.585	1.165	.466
0.8	0	0.188	0.546	0.411	0.700	0.726	0.738
	30	.301	.596	.594	.692	.945	.671
	60	.337	.637	.660	.713	1.033	.648
	90	.340	.658	.668	.724	1.042	.637

(e) h = 10.0

ξ_o	α, deg	SR for Z = 1.0	DR for Z = 1.0	SR for Z = 2.0	DR for Z = 2.0	SR for Z = 4.0	DR for Z = 4.0
0.2	0	0.085	0.554	0.200	0.807	0.354	0.978
	30	.186	.631	.432	.795	.790	.795
	60	.384	.595	.737	.615	1.131	.520
	90	.429	.648	.800	.664	1.200	.548
0.4	0	0.193	0.582	0.414	0.735	0.688	0.756
	30	.256	.587	.533	.694	.885	.656
	60	.374	.601	.721	.630	1.106	.530
	90	.381	.717	.748	.739	1.150	.596
0.8	0	0.289	0.563	0.578	0.650	0.920	0.634
	30	.304	.601	.608	.686	.971	.648
	60	.345	.635	.680	.689	1.064	.608
	90	.338	.716	.687	.766	1.087	.647

The ratio of scattered power to incident power $\left(SR = \frac{P_S}{P_I}\right)$ varied from about 0.04 to over 1.0. It was a minimum for grazing incidence ($\alpha = 0^o$) and a maximum for normal incidence ($\alpha = 90^o$) and increased monotonically with real impedance (resistance). As the resistance becomes infinite, SR must approach the value for the hard cylinder. A computation was made for the case of the hard cylinder and checked by using tabulated values of the radial functions (ref. 17). The numerical result for scattered power was found to be correct for $h = 2.0$ and $\alpha = 0^o$.

The ratio of the dissipated power to the incident power $\left(DR = \frac{P_d}{P_I}\right)$ must have a maximum value between $Z = 0$ and $Z = \infty$. The value of DR depends on the product of the pressure drop and velocity at the cylinder surface. For zero resistance the pressure drop is zero, and for infinite resistance the velocity is zero whereas the pressure differential must remain finite. It may be seen from the table that the optimum (maximum-dissipation) resistance is usually around 2, except for grazing incidence on a thin ($\xi_o = 0.2$) cylinder where it is near 4. This large value of optimum resistance is a surprising result, since in one-dimensional problems, a resistive impedance of 1 gives the maximum absorption. For thin cylinders DR was an increasing function of the angle of incidence for $Z = 1.0$ and a decreasing function of the angle for $Z = 4.0$. Another interesting result is that the maximum value for DR is just slightly larger than 1 for grazing incidence on a thin cylinder. Thus, it may be concluded that the maximum percentage of energy which can be removed from sound propagating in a duct is equal to the percentage of duct area blocked by the splitter rings and spokes.

In the case of normal incidence, the dissipation by an elliptic cylinder with eccentricity of nearly 1 should be roughly comparable to the dissipation by infinite parallel planes of porous material. If the length of the minor axis is held constant while the major axis is made much longer, then two sides of the cylinder will become nearly straight and parallel. This comparison is illustrated in figure 2. The data in this figure are for $\xi_o = 0.2$, which corresponds to a cylinder whose major axis is roughly five times the length of the minor axis. The ratio of the dissipated power to the power in the normally incident plane wave is plotted against h, which may be interpreted as a frequency parameter, for the condition of normal incidence. The curves in figure 2 give this ratio for parallel planes whose spacing is equal to the length of the minor axis of the cylinder. The maximum dissipation and minimum dissipation for the parallel planes occur at very nearly the same frequencies as the maximum and minimum points for the cylinder, and the maxima have nearly the same values.

Data for grazing incidence are also shown in figure 2. Only about one-fifth as much energy is dissipated from the grazing waves as from the normally incident wave. Dissipation ratios for the grazing incidence waves are shown in figure 3. The maximum and

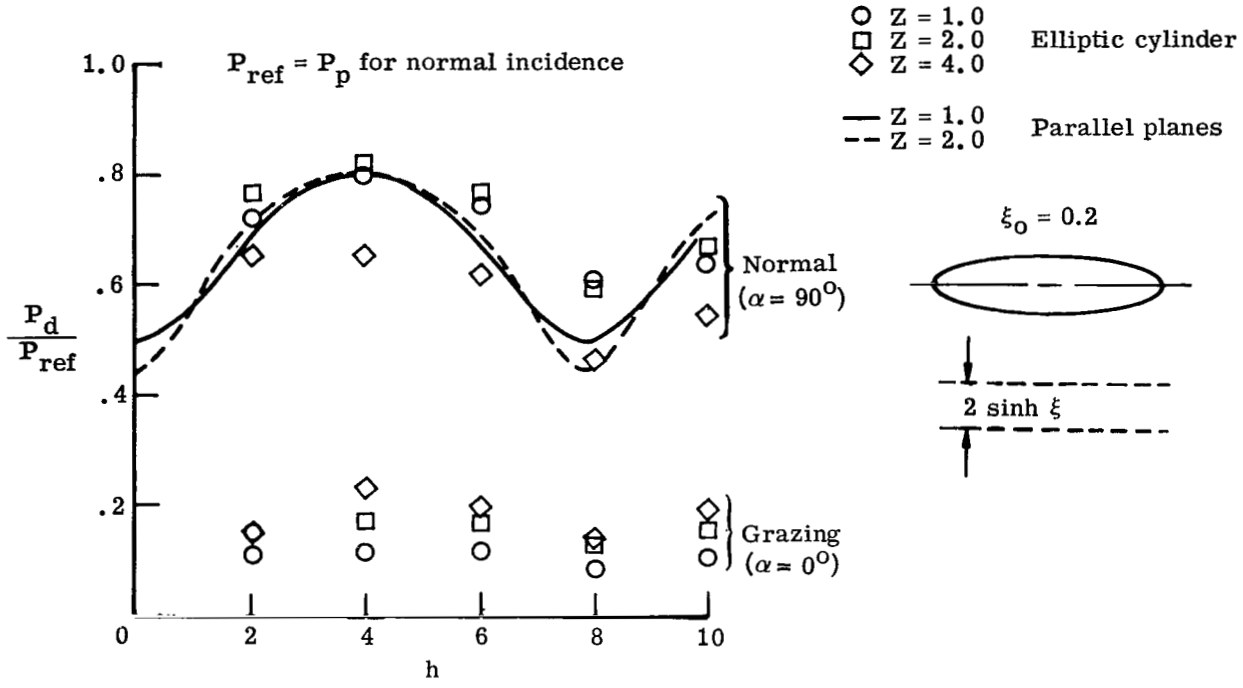

Figure 2.- Comparison of dissipation by elliptic cylinder and parallel planes.

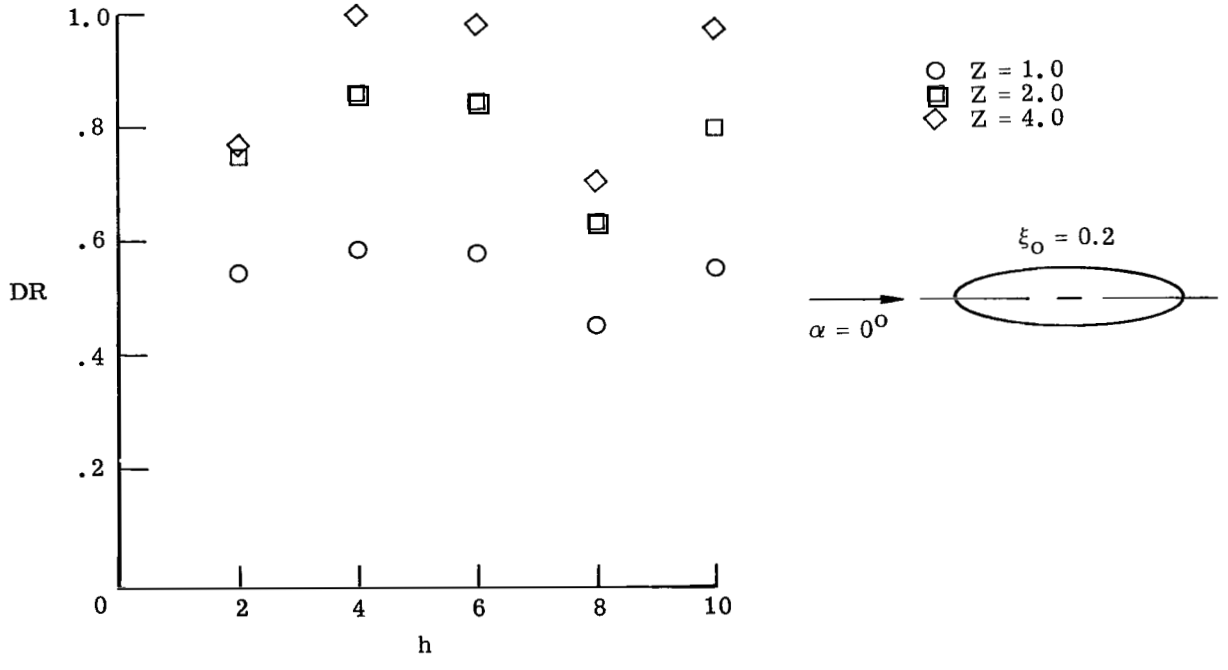

Figure 3.- Dissipation ratio for grazing incidence.

minimum values of DR occur at frequencies which correspond to the frequencies at which the maxima and minima occur for the normal-incidence condition, a result which indicates that the minor-axis length is the critical dimension for grazing-wave energy dissipation. The maximum dissipation occurs when the minor axis is about one-fourth wavelength.

CONCLUDING REMARKS

The exact solution for scattering from a porous elliptic cylindrical shell with linear acoustic impedance has been found in terms of Mathieu function series. Coefficients of these series are solutions of four infinite matrix equations. Elements of the matrices depend on integrals of the periodic Mathieu functions and on the radial Mathieu functions. Series expressions for the integrals have been found. The Mathieu functions may be evaluated in terms of known trigonometric and Bessel function series. By use of highly accurate modern computers, it has been possible to evaluate these functions for a range of parameters for which no tables are available. Thus, it has been possible to present results for a range of frequencies for which only formal solutions exist in previous literature.

For a special case in which the acoustic impedance is a certain function of position on the cylinder, the infinite matrices reduce to diagonal forms, so that simple closed-form expressions in the series solutions are available.

It is possible to obtain numerical results inside and outside of the cylinder in both the near field and the far field. Near-field solutions have been used to obtain the power dissipated in the porous shell.

The periodic Mathieu functions used in this paper could easily be evaluated to eight significant figures. The radial Mathieu functions were more difficult to evaluate. The Bessel function series was superior for evaluating the radial Mathieu function of the first kind. This series had the property that higher order functions were more accurate for larger values of the parameter s (the square of the dimensionless focal length). Since s is proportional to frequency-squared, this property makes it possible to find solutions at the higher frequencies when the higher order functions are needed.

The Bessel function product series was superior for computing the radial Mathieu function of the second kind. The accuracy of this series decreased with increasing s, or frequency. The complex radial Mathieu function was computed to six significant figures in the range $4 \leqq s \leqq 100$.

The integrals which give the coupling terms in the scattering equation were evaluated by double infinite series to eight significant figures.

A study of scattering and dissipation of energy by the porous cylindrical shell has been made. Scattering is negligible for grazing incidence on the cylinder and is always

a maximum for normal incidence. The scattering increases monotonically with resistance of the porous material.

The energy dissipated varies with frequency and resistance. The maximum dissipation usually occurs near a resistance of about 2; however, for grazing incidence the maximum dissipation occurs near a resistance of 4.

The ratio of dissipated energy to incident energy reaches a maximum of about 1 for the grazing-incidence condition. This maximum dissipation occurs when the minor axis of the cylinder is about one-fourth wavelength. This result suggests that the maximum percentage of energy which can be removed by placing a splitter in a duct is numerically equal to the percentage of duct area blocked by the splitter.

Langley Research Center,
National Aeronautics and Space Administration,
Hampton, Va., June 21, 1971.

APPENDIX

EVALUATION OF COUPLING COEFFICIENTS

The integrals $M_{l,r}$ and $N_{l,r}$ from equations (23) to (26) are defined as

$$M_{l,r} = \frac{2}{h}\int_0^{2\pi} \frac{Se_l(\eta)Se_r(\eta)d\eta}{\sqrt{2(\cosh 2\xi_o - \cos 2\eta)}} \tag{38}$$

and

$$N_{l,r} = \frac{2}{h}\int_0^{2\pi} \frac{So_l(\eta)So_r(\eta)d\eta}{\sqrt{2(\cosh 2\xi_o - \cos 2\eta)}} \tag{39}$$

In order to evaluate the integrals, each term in the integrand will be expanded as a Fourier series in the variable η as follows:

$$Se_{2r}(\eta) = \sum_{k=0}^{\infty} De_{2k}^{(2r)} \cos 2k\eta \tag{40}$$

$$Se_{2r+1}(\eta) = \sum_{k=0}^{\infty} De_{2k+1}^{(2r+1)} \cos(2k+1)\eta \tag{41}$$

$$So_{2r+1}(\eta) = \sum_{k=0}^{\infty} Do_{2k+1}^{(2r+1)} \sin(2k+1)\eta \tag{42}$$

$$So_{2r+2}(\eta) = \sum_{k=0}^{\infty} Do_{2k+2}^{(2r+2)} \sin(2k+2)\eta \tag{43}$$

When these series are substituted into equations (38) and (39) for term-by-term integration, it will be necessary to evaluate the integral

$$I_m = \int_0^{2\pi} \frac{\cos m\eta \, d\eta}{\sqrt{2(\cosh 2\xi_o - \cos 2\eta)}} \tag{44}$$

The radical in the integrand of equation (44) may be represented as a series of Gegenbauer polynomials. Rainville (ref. 19) gives the generating function definition of these polynomials as

$$\left(1 - 2xt + t^2\right)^{-\nu} = \sum_{n=0}^{\infty} C_n^{\nu}(x)t^n \tag{45}$$

The denominator of the integrand in equation (44) may be written as

$$\left[2\left(\cosh 2\xi_o - \cos 2\eta\right)\right]^{-1/2} = \left[e^{2\xi_o}\left(1 - 2\cos 2\eta e^{-2\xi_o} + e^{-4\xi_o}\right)\right]^{-1/2} \tag{46}$$

Therefore

$$\left[2\left(\cosh 2\xi_o - \cos 2\eta\right)\right]^{-1/2} = e^{-\xi_o} \sum_{n=0}^{\infty} C_n^{1/2}(\cos 2\eta)e^{-2n\xi_o} \tag{47}$$

The Gegenbauer polynomial in equation (47) may be given as (ref. 19, p. 283)

$$C_n^{1/2}(\cos 2\eta) = \sum_{k=0}^{n} \frac{\left(\frac{1}{2}\right)_k \left(\frac{1}{2}\right)_{n-k} \cos 2(n - 2k)\eta}{k!(n - k)!} \tag{48}$$

where $\left(\frac{1}{2}\right)_k = \left(\frac{1}{2}\right)\left(\frac{3}{2}\right) \cdots \left(k - \frac{1}{2}\right)$.

Equations (47) and (48) combined give the desired expansion for the radical:

$$\left[2\left(\cosh 2\xi_o - \cos 2\eta\right)\right]^{-1/2} = e^{-\xi_o} \sum_{n=0}^{\infty} e^{-2n\xi_o} \sum_{k=0}^{n} \frac{\left(\frac{1}{2}\right)_k \left(\frac{1}{2}\right)_{n-k} \cos 2(n - 2k)\eta}{k!(n - k)!} \tag{49}$$

From equation (49) it may be seen that the integral in equation (44) is zero for all odd values of m; consequently, the only integrals which it is necessary to evaluate are of the form

$$I_{2m} = \int_0^{2\pi} \frac{\cos 2m\eta \, d\eta}{\sqrt{2\left(\cosh 2\xi_o - \cos 2\eta\right)}} \tag{50}$$

Substituting equation (49) into equation (50) gives

$$I_{2m} = e^{-\xi_o} \sum_{n=m}^{\infty} e^{-2n\xi_o} \sum_{k=0}^{n} \frac{\left(\frac{1}{2}\right)_k \left(\frac{1}{2}\right)_{n-k}}{k!(n-k)!} \int_0^{2\pi} \cos 2(n-2k)\eta \cos 2m\eta \, d\eta \tag{51}$$

That is,

$$I_{2m} = e^{-(2m+1)\xi_o} \sum_{p=0}^{\infty} \sum_{k=0}^{m+2p} \frac{\left(\frac{1}{2}\right)_k \left(\frac{1}{2}\right)_{(m+2p-k)}}{k!(m+2p-k)!} e^{-4p\xi_o} \int_0^{2\pi} \cos 2(m+2p-2k)\eta \cos 2m\eta \, d\eta \tag{52}$$

In equation (52) nonzero terms occur only when $k = p$ or $k = p + m$; therefore,

$$I_{2m} = 2\pi e^{-(2m+1)\xi_o} \sum_{p=0}^{\infty} \frac{\left(\frac{1}{2}\right)_p \left(\frac{1}{2}\right)_{p+m}}{p!(p+m)!} e^{-4p\xi_o} \tag{53}$$

Since the factorial terms in equation (53) form a decreasing sequence, the error due to truncating the series is

$$E < \int_N^{\infty} \frac{\left(\frac{1}{2}\right)_p \left(\frac{1}{2}\right)_{p+m}}{p!(p+m)!} e^{-4p\xi_o} dp < \frac{\left(\frac{1}{2}\right)_N \left(\frac{1}{2}\right)_{N+m}}{N!(N+m)!} \frac{e^{-4N\xi_o}}{4\xi_o} < \frac{e^{-4N\xi_o}}{4\xi_o} \tag{54}$$

where N is the number of required terms.

If an error less than e^{-F} is desired when $4\xi_o \ll 1$, an estimate of the number of required terms is

$$N > \frac{F - \ln 4\xi_o}{4\xi_o} \tag{55}$$

where F is the number of significant figures. With N determined by equation (55), equation (53) becomes

$$I_{2m} \approx 2\pi e^{-(2m+1)\xi_o} \sum_{p=0}^{N} \frac{\left(\frac{1}{2}\right)_p \left(\frac{1}{2}\right)_{p+m}}{p!(p+m)!} e^{-4p\xi_o} \tag{56}$$

Once the integrals I_{2m} are evaluated, they may be used to evaluate the integrals in equations (38) and (39). First, consider the product of the Mathieu functions in the integrand of equation (38). If Se_l and Se_r both have period π, their product may be written as

$$Se_{2l}Se_{2r} = \sum_{k=0}^{\infty} \sum_{j=0}^{\infty} De_{2k}^{(2l)} De_{2j}^{(2r)} \cos 2k\eta \cos 2j\eta \tag{57}$$

Since $\cos 2k\eta \cos 2j\eta = \frac{1}{2} \cos 2(k - j)\eta + \frac{1}{2} \cos 2(k + j)\eta$, the argument of each term in the series is an even multiple of η. Consequently,

$$M_{2l,2r} = \frac{2}{h} \sum_{k=0}^{\infty} \sum_{j=0}^{\infty} De_{2k}^{(2l)} De_{2j}^{(2r)} \left[\frac{I_{2|k-j|} + I_{2(k+j)}}{2}\right] \tag{58}$$

The product of Mathieu functions with different periods gives a series whose terms are all odd multiples of η. It was noted previously that the integral of these terms is zero; therefore,

$$M_{2l+1,2r} = 0 \tag{59}$$

and

$$M_{2l,2r+1} = 0 \tag{60}$$

The product of even Mathieu functions with period 2π is

$$Se_{2l+1}Se_{2r+1} = \sum_{k=0}^{\infty} \sum_{j=0}^{\infty} De_{2k+1}^{(2l+1)} De_{2j+1}^{(2r+1)} \cos(2k + 1)\eta \cos(2j + 1)\eta \tag{61}$$

Therefore

$$M_{2l+1,2r+1} = \frac{2}{h} \sum_{k=0}^{\infty} \sum_{j=0}^{\infty} De_{2k+1}^{(2l+1)} De_{2j+1}^{(2r+1)} \left[\frac{I_{2|k-j|} + I_{2(k+j+1)}}{2}\right] \tag{62}$$

A similar evaluation for integrals involving odd Mathieu functions gives

$$N_{2\ell+1,2r+1} = \frac{2}{h} \sum_{k=0}^{\infty} \sum_{j=0}^{\infty} Do_{2k+1}^{(2\ell+1)} Do_{2j+1}^{(2r+1)} \left[\frac{I_{2|k-j|} - I_{2(k+j+1)}}{2} \right] \tag{63}$$

$$N_{2\ell+2,2r+2} = \frac{2}{h} \sum_{k=0}^{\infty} \sum_{j=0}^{\infty} Do_{2k+2}^{(2\ell+2)} Do_{2j+2}^{(2r+2)} \left[\frac{I_{2|k-j|} - I_{2(k+j+2)}}{2} \right] \tag{64}$$

$$N_{2\ell+1,2r} = 0 \tag{65}$$

and

$$N_{2\ell+2,2r+1} = 0 \tag{66}$$

REFERENCES

1. Marsh, Alan H.: Study of Acoustical Treatments for Jet-Engine Nacelles. J. Acoust. Soc. Amer., vol. 43, no. 5, May 1968, pp. 1137-1156.

2. Bouwkamp, C. J.: Diffraction Theory. Reports on Progress in Physics, Vol. XVII, Phys. Soc. (London), 1954, pp. 35-100.

3. Morse, Philip M.; and Ingard, K. Uno: Theoretical Acoustics. McGraw-Hill Book Co., Inc., c.1968, pp. 458-462.

4. Yeh, C.: The Diffraction of Waves by a Penetrable Ribbon. J. Math. Phys. (N.Y.), vol. 4, no. 1, Jan. 1963, pp. 65-71.

5. Barakat, Richard: Diffraction of Plane Waves by an Elliptic Cylinder. J. Acoust. Soc. Amer., vol. 35, no. 12, Dec. 1963, pp. 1990-1996.

6. Barakat, Richard; Houston, Agnes; and Levin, Elgie: Power Series Expansions of Mathieu Functions With Tables of Numerical Results. J. Math. Phys., vol. XLII, no. 3, Sept. 1963, pp. 200-247.

7. Burke, James E.: Low-Frequency Approximations for Scattering by Penetrable Elliptic Cylinders. J. Acoust. Soc. Amer., vol. 36, no. 11, Nov. 1964, pp. 2059-2070.

8. Burke, J. E.; and Twersky, V.: On Scattering of Waves by an Elliptic Cylinder and by a Semielliptic Protuberance on a Ground Plane. J. Opt. Soc. Amer., vol. 54, no. 6, June 1964, pp. 732-744.

9. Twersky, Victor: Acoustic Bulk Parameters of Random Volume Distributions of Small Scatterers. J. Acoust. Soc. Amer., vol. 36, no. 7, July 1964, pp. 1314-1329.

10. Wiltse, James C.; and King, Marcia J.: Values of the Mathieu Functions. Tech. Rep. No. AF-53 (Contract No. AF 33(616)-3374), Radiat. Lab., Johns Hopkins Univ., Aug. 1958.

11. King, Marcia J.; and Wiltse, James C.: Derivatives, Zeros, and Other Data Pertaining to Mathieu Functions. Tech. Rep. No. AF-57 (Contract No. AF 33(616)-3374), Radiat. Lab., Johns Hopkins Univ., Dec. 1958.

12. Anon.: Tables Relating to Mathieu Functions – Characteristic Values, Coefficients, and Joining Factors. Nat. Bur. Stand., Appl. Math. Ser. 59, U.S. Dep. Com., Aug. 1, 1967.

13. McLachlan, N. W.: Theory and Application of Mathieu Functions. Dover Publ., Inc., c.1964.

14. Arscott, F. M.: Periodic Differential Equations. The Macmillan Co., 1964.

15. Blanch, Gertrude: On the Computation of Mathieu Functions. J. Math. Phys., vol. XXV, no. 1, Feb. 1946, pp. 1-20.

16. Stegun, Irene A.; and Abramowitz, Milton: Generation of Bessel Functions on High Speed Computers. Math. Tables Aids Comput., vol. XI, no. 60, Oct. 1957, pp. 255-257.

17. Blanch, G.; and Clemm, D. S.: Tables Relating to the Radial Mathieu Functions. Aeronaut. Res. Lab., U.S. Air Force, 1965.
Vol. 1 – Functions of the First Kind.
Vol. 2 – Functions of the Second Kind.

18. Kantorovich, L. V.; and Krylov, V. I. (Curtis D. Benster, trans.): Approximate Methods of Higher Analysis. P. Noordhoff Ltd. (Groningen), 1958.

19. Rainville, Earl D.: Special Functions. The Macmillan Co., c.1960.

NASA-Langley, 1971 —— 23 L-7668

"The aeronautical and space activities of the United States shall be conducted so as to contribute . . . to the expansion of human knowledge of phenomena in the atmosphere and space. The Administration shall provide for the widest practicable and appropriate dissemination of information concerning its activities and the results thereof."

— NATIONAL AERONAUTICS AND SPACE ACT OF 1958

NASA SCIENTIFIC AND TECHNICAL PUBLICATIONS

TECHNICAL REPORTS: Scientific and technical information considered important, complete, and a lasting contribution to existing knowledge.

TECHNICAL NOTES: Information less broad in scope but nevertheless of importance as a contribution to existing knowledge.

TECHNICAL MEMORANDUMS: Information receiving limited distribution because of preliminary data, security classification, or other reasons.

CONTRACTOR REPORTS: Scientific and technical information generated under a NASA contract or grant and considered an important contribution to existing knowledge.

TECHNICAL TRANSLATIONS: Information published in a foreign language considered to merit NASA distribution in English.

SPECIAL PUBLICATIONS: Information derived from or of value to NASA activities. Publications include conference proceedings, monographs, data compilations, handbooks, sourcebooks, and special bibliographies.

TECHNOLOGY UTILIZATION PUBLICATIONS: Information on technology used by NASA that may be of particular interest in commercial and other non-aerospace applications. Publications include Tech Briefs, Technology Utilization Reports and Technology Surveys.

Details on the availability of these publications may be obtained from:

SCIENTIFIC AND TECHNICAL INFORMATION OFFICE

NATIONAL AERONAUTICS AND SPACE ADMINISTRATION

Washington, D.C. 20546